Frontiers in Bioscience Landmark

Front. Biosci. (Landmark Ed) **2023**; 28(12): 341
https://doi.org/10.31083/j.fbl2812341

Original Research

Exploration of the Pharmacological Mechanism of Vitexicarpin against Triple-Negative Breast Cancer in Network Pharmacology

Tianhui Wu[1,†], Min Xiang[2,*,†], Yujiao Li[1], Yahan Gao[2], Da Teng[1], Minxuan Sun[3], Weiqiang Guo[1,*], Yuanshuai Zhou[3,*]

[1]School of Chemistry and Life Science, Suzhou University of Science and Technology, 215000 Suzhou, Jiangsu, China
[2]School of Medicine, Suzhou Vocational Health College, 215000 Suzhou, Jiangsu, China
[3]Institute of Medical Biotechnology, Suzhou Institute of Biomedical Engineering and Technology, 215000 Suzhou, Jiangsu, China
*Correspondence: xiangmin99@126.com (Min Xiang); weiqiang.guo@hotmail.com (Weiqiang Guo); zhouys@sibet.ac.cn (Yuanshuai Zhou)
†These authors contributed equally.

Academic Editor: Marco Falasca
Submitted: 19 July 2023 Revised: 14 September 2023 Accepted: 27 September 2023 Published: 26 December 2023

Abstract

Background: Vitexicarpin (VIT), an isoflavone derived from various medicinal herbs, has shown promising anti-tumor activities against multiple cancer cells. However, the understanding of the mechanisms and potential targets of VIT in treating triple-negative breast cancer (TNBC) remains limited. **Methods**: The potential VIT targets were searched for in the Super-PRED online database, while the TNBC targets were acquired in the DisGeNET database, and the Veeny database was used to identify the VIT and TNBC targets that overlapped. Then, GO and KEGG enrichment analyses were carried out in the DAVID database. The protein–protein interaction (PPI) network was constructed to acquire the hub targets in the STRING database, and the overall survival analysis of the hub targets was examined in the Kaplan–Meier plotter database. Afterward, molecular docking was performed to evaluate the binding capabilities between VIT and the hub targets. In order to measure the effect of VIT on proliferation, apoptosis, and cell cycle arrest in the TNBC cell lines—MDA-MB-231 and HCC-1937—the Cell Counting Kit-8 (CCK-8) assay and flow cytometry analysis were performed. The Western blot and pull-down assays were used to verify the molecular mechanisms by modulating the hub targets. **Results**: The network pharmacology results identified a total of 37 overlapping genes that were shared by VIT and TNBC. The results of the PPI network and molecular docking analyses showed that HSP90AA1, CREBBP, and HIF-1A were key targets of VIT against TNBC. However, the pull-down results suggested that VIT could directly bind to HSP90AA1 and HIF-1A, yet not to CREBBP. The results of the *in vitro* tests showed that VIT decreased proliferation and induced apoptosis in MDA-MB-231 and HCC-1937 cells, in a dose-dependent manner, while the cell cycle arrest occurred at the G2 phase. Mechanistically, the Western blot assay demonstrated that VIT decreased the expression of HSP90AA1, CREBBP, and HIF-1A. **Conclusions**: VIT inhibited growth and induced apoptosis of TNBC cells by modulating HIF-1A, HSP90AA1, and CREBBP expression. Our findings suggest that VIT is a potential drug for TNBC therapy.

Keywords: vitexicarpin; triple-negative breast cancer; network pharmacology; HSP90AA1; CREBBP; HIF-1A

1. Introduction

Breast cancer (BRCA) is a prevalent disease that affects women's health on a global scale. Among BRCA patients, more than 20% are diagnosed with triple-negative breast cancer (TNBC), which has the clinical characteristics of high metastasis and poor prognosis [1,2]. Additionally, TNBC has features such as the loss of the estrogen receptor (ER), progesterone receptor (PR), and human epidermal growth factor receptor-2 (HER2). Due to its clinical features, TNBC lacks any effective therapeutic strategies and drugs [3,4]. Hence, there is an urgent need to explore novel therapeutic strategies and drugs to reduce TNBC recurrence.

Vitexicarpin (5,7,4-trihydroxyflavone-8-glucoside, VIT), an isoflavone compound (Fig. 1A), is widely distributed in various traditional Chinese medicinal herbs, including pearl millet, hawthorn, and pigeon pea. Extensive research has demonstrated that VIT possesses multiple functions, including anti-inflammatory, antioxidant, and anti-tumor [5,6]. It has been found that VIT inhibits glioblastoma and non-small cell lung cancer (NSCLC) by blocking the PI3K/AKT/mTOR pathway [7]. However, the mechanisms through which VIT exerts these effects and its potential inhibitory targets in TNBC are yet to be fully understood.

Over the past few decades, network pharmacology and bioinformatics analyses have provided researchers with valuable tools to study the mechanism of natural compounds [8]. Thus, in our research, we sought to evaluate the possible targets and mechanisms of VIT in TNBC treatment. Furthermore, *in vitro* experiments were conducted to validate these findings. This study presents a novel approach against TNBC.

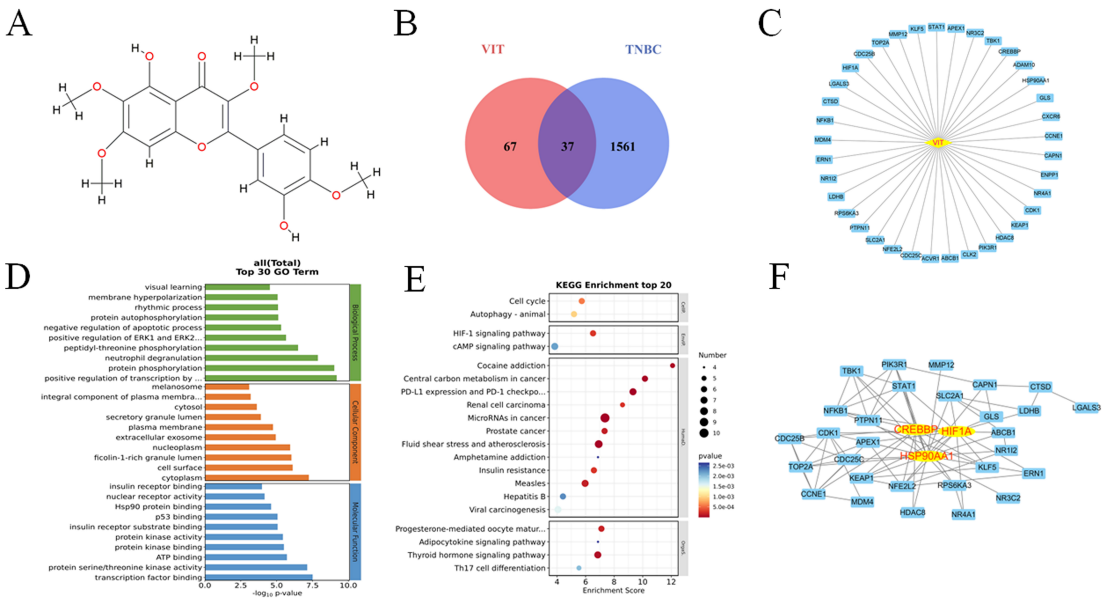

Fig. 1. Network pharmacology and biological function analysis of vitexicarpin (VIT) therapy for triple-negative breast cancer (TNBC). (A) VIT construct. (B) Venn diagram of the TNBC and VIT target genes. (C) VIT-related TNBC target genes network. (D) The top 30 enriched Gene Ontology (GO) terms. (E) The top 20 enriched Kyoto Encyclopedia of Genes and Genomes (KEGG) pathways and processes. (F) Protein–protein interaction (PPI) network analyzed by Search Tool for Recurring Instances of Neighbouring Genes (STRING), the hub genes are indicated in red.

2. Materials and Methods

2.1 Chemicals and Antibodies

VIT was purchased from the National Institute for the Control of Pharmaceutical and Biological Products (111554, NICPBP, Beijing, China). TNBC cell lines, MDA-MB-231 and HCC-1937, were obtained from the Cell Bank of the Chinese Academy of Science (Shanghai, China). All cell lines were validated by STR profiling and tested negative for mycoplasma (C0298S, Beyotime, Shanghai, China). Cells were all cultured in a humidified incubator at 37 °C and 5% CO_2. DMEM, RPMI-1640, and FBS were purchased from Gibco (12800082, 31800089, 16140071, Gibco, New York, USA). Specific antibodies for β-actin, HSP90AA1, CREBBP, and HIF-1A were purchased from the Proteintech group (20536-1-AP, 22277-1-AP, 20960-1-AP, Proteintech, Wuhan, China). Primary Antibody of HSP90AA1 was purchased from Beyotime (AF7140, Beyotime, Shanghai, China). Chemicals, such as SDS, and glycine for Western immunoblots were acquired from Beyotime Co, Ltd. (ST626, ST085, Beyotime, Shanghai, China).

2.2 Predicting VIT Targets

The VIT targets were predicted using the online Super-PRED server (https://prediction.charite.de/subpages/target_prediction.php). Subsequently, we searched for these candidate targets in the UniProt database (https://www.uniprot.org) to identify which proteins interacted with VIT.

2.3 Collecting Related Targets of TNBC

We collected TNBC-related genes from DisGeNET (https://www.disgenet.org/) and the Comparative Toxicogenomics database (http://ctdbase.org/) by using the keyword: “triple-negative breast cancer”. After removing repetitive targets, we obtained a list of insomnia targets. We identified the overlapping genes for VIT and TNBC using Veeny 2.1 (https://bioinfogp.cnb.csic.es/tools/venny/).

2.4 Constructing the “VIT–TNBC-Related Genes” Network

To visualize the relationship between VIT and TNBC, we used Cytoscape software 3.6 (San Diego, CA, USA) to create a network diagram based on the 37 overlapping genes obtained from integrating the potential targets of VIT with the TNBC-related genes.

2.5 GO and KEGG Pathway Enrichment Analyses

To explore the impact of VIT on TNBC treatment, we performed GO and KEGG pathway enrichment analyses using the DAVID database (https://david.ncifcrf.gov/). The results of the GO and KEGG pathway enrichment analyses were visualized using R software 4. 2. 1 (R&R Software Co. Ltd., Budapest 1038, Hungary).

2.6 Protein–Protein Interaction (PPI) Network Analysis

To investigate the interaction of the overlapping targets of VIT, a PPI network was generated using the STRING database (https://string-db.org/). The minimum interaction score required was set at $\geq$0.4, using the default parameters. The resulting PPI network was visualized using Cytoscape software 3.6 (San Diego, CA, USA).

2.7 Molecular Docking Analysis of VIT and TNBC-Related Targets

The VIT 3D structure (No: 5280441) was from PubChem (https://pubchem.ncbi.nlm.nih.gov/) and inputted into Open Babel software 3.1.1 (Pittsburgh, USA) to generate the mol2 formula. The HSP90AA1 (5H22), HIF-1A (3KCX), and CREBBP (4TQN) crystal structures were obtained from Protein Data Bank (https://www.rcsb.org). Subsequently, the water and ligand molecules were removed from the 3D structures using Discovery Studio 4.5 (Omaha, Nebraska, USA). The molecular docking analysis of VIT and its potential targets was performed using Discovery Studio to predict their interaction activity.

2.8 Kaplan–Meier Test

Survival information of the VIT hub genes following TNBC treatment was obtained by the Kaplan–Meier plotter (http://kmplot.com/analysis/), which was established based on the microarray and RNA-seq datasets for TNBC from TGCA [9].

2.9 Cell Culture

MDA-MB-231 cells were cultured in DMEM, while HCC-1937 were cultured in RPMI-1640. Both these cell lines were supplemented with 10% FBS and 1% penicillin/streptomycin. The cells were maintained at 37 °C in a humidified atmosphere containing 5% CO_2.

2.10 Cell Viability Assay

MDA-MB-231 and HCC-1937 cells were seeded into separate 96-well plates and treated with different doses of VIT for 24, 48, and 72 h, respectively. Then, the cells were withdrawn from the media and incubated with Cell Counting Kit-8 (CCK-8) (CT0001, Sparkjade, Qingdao, China) reagents at 37 °C for 4 h. Thereafter, the absorbance of each well was instantly measured at 450 nm using an ELISA microplate reader (TECAN Infinite F50, Männedorf, Switzerland). The cell viability rates were calculated after normalizing them to the control group.

2.11 Apoptosis Analysis

MDA-MB-231 and HCC-1937 cells were incubated with VIT for 24 hours, while groups without VIT were established as the corresponding negative controls. Secondly, cells were rinsed twice with pre-chilled PBS, and then stained with the Annexin V Apoptosis Detection kit (640932, BioLegend, San Diego, CA, USA). Finally, the cells were analyzed by flow cytometry. Apoptosis was determined based on the percentage of cells binding with Annexin V+/PI+. The results are the average values obtained from three separate experiments.

2.12 Cell Cycle Analysis

After treatment with VIT for 24 h, MDA-MB-231 and HCC-1937 cells were collected and washed with pre-chilled PBS before being fixed overnight at 4 °C with 70% ice-cold ethanol. After washing with PBS, the cells were stained with a solution containing 50 µg/mL PI and 1 mg/mL RNase A and incubated in the dark for 30 min at 37 °C. Analysis of the cell cycle distribution was performed by flow cytometry.

2.13 Pull-Down Assay

To perform the pull-down assay, VIT (5 µmol) was coupled to CNBr-activated Sepharose 4B (GE Healthcare Bio-Sciences Corp,, Piscataway, USA) matrix beads (0.1 g) in 500 µL 0.1 M $NaHCO_3$ pH 8.3 solution containing 0.5 M NaCl and 40% DMSO (pH 8.0) and incubated overnight at 4 °C, in accordance with the manufacturer's instructions. Then, the total MDA-MB-231 cell lysates were incubated overnight in the reaction buffer (50 mM Tris pH7.5, 5 mM EDTA, 150 mM NaCl, 1 mM DTT, 0.01% NP-40, 2 µg/mL BSA) with either Sepharose 4B–VIT or Sepharose 4B alone, with gentle rocking at 4 °C. Finally, the binding was determined by Western immunoblotting.

2.14 Western Blot

MDA-MB-231 and HCC-1937 cells were treated with VIT for 24 h. The following day, the cells were harvested, washed with ice-cold PBS, and lysed on ice for 15 min in RIPA lysis buffer containing protease inhibitors. Then, the lysates were centrifuged at 12,000 g for 20 min at 4 °C. The protein concentrations were measured using a BCA assay kit (P0010, Beyotime, Shanghai, China). Equal amounts of total protein were loaded and separated on an 8% SDS-PAGE gel before being transferred to a PVDF membrane. The blots were blocked in 5% non-fat milk for 1 hour at room temperature and then incubated with primary antibodies targeting either CREBBP, HSP90AA1, or HIF-1A, overnight at 4 °C. Subsequently, the blots were incubated with HRP (horseradish peroxidase)-conjugated secondary antibodies. Finally, the protein bands were visualized using an electrochemiluminescence detection system (Odyssey® Fc, Lincoln, Nebraska, USA). The levels of the detected proteins were normalized to β-actin.

Table 1. The 37 potential VIT targets in the treatment of TNBC.

No.	Gene	ABBR	No.	Gene	ABBR
1	*APEX1*	APE; APX; APE1	20	*HDAC8*	HD8; WTS; RPD3
2	*KLF5*	CKLF; IKLF; BTEB2	21	*KEAP1*	INrf2; KLHL19
3	*TOP2A*	TOP2; TP2A; TOPIIA	22	*CDK1*	CDC2; CDC28A
4	*HIF1A*	HIF1; MOP1; PASD8;	23	*NR4A1*	HMR; TR3; NP10
5	*CTSD*	CPSD; CLN10; HEL-S-130P	24	*ENPP1*	M6S1; NPP1; NPPS
6	*NFKB1*	KBF1; EBP-1; NF-kB	25	*CAPN1*	muCL; CANP1
7	*MDM4*	HDMX; MDMX; MRP1	26	*CCNE1*	cyclinE1
8	*ERN1*	IRE1; IRE1P; IRE1a	27	*CXCR6*	BONZO; CD186
9	*NR1I2*	BXR; PAR; PRR	28	*GLS*	GAC; GAM; KGA
10	*LDHB*	LDH-B; LDH-H; LDHBD	29	*HSP90AA1*	EL52; HSPN; LAP2
11	*RPS6KA3*	CLS; HU-3; RSK2	30	*ADAM10*	RAK; kuz; AD10
12	*PTPN11*	CFC; NS1; JMML; SHP2	31	*CREBBP*	CBP; RSTS; KAT3A
13	*SLC2A1*	CSE; PED; DYT9	32	*TBK1*	NAK; T2K; IIAE8
14	*NFE2L2*	NRF2; HEBP1; Nrf-2;	33	*NR3C2*	MR; MCR; MLR
15	*CDC25C*	CDC25; PPP1R60	34	*STAT1*	CANDF7; IMD31A
16	*ACVR1*	FOP; ALK2; SKR1; TSRI	35	*MMP12*	HME; MMP-12
17	*ABCB1*	CLCS; MDR1; P-GP	36	*CDC25B*	
18	*CLK2*		37	*LGALS3*	L31; GAL3; MAC2
19	*PIK3R1*	p85; AGM7; GRB1			

2.15 Statistical Analysis

Statistical analysis was conducted using Origin 8.0 (Northampton, Massachusetts, USA), and the data are presented as mean $\pm$ SD. The *t*-test was used for pairwise comparison, with statistical significance considered as $p < 0.05$ (*) and as highly significant at $p < 0.01$ (**).

3. Results

3.1 TNBC-Related Targets from VIT Predictions and Analysis

We conducted an analysis to identify potential VIT target genes for the treatment of TNBC. Firstly, to investigate the potential targets of VIT in TNBC, we utilized the Super-PRED database, which predicted 105 candidate genes (**Supplementary File 1**) as potential targets for VIT. In addition, we retrieved a list of 1588 TNBC-related targets from the DisGeNET database (**Supplementary File 2**).

A total of 37 overlapping targets were identified by expressing these two target clusters in a Venn diagram (Fig. 1B and Table 1). To visualize the relationship between VIT and the TNBC-related targets, we constructed a network known as the 'VIT–TNBC-related targets' network (Fig. 1C), which consisted of 38 nodes that represented the genes and 37 edges that depicted the connections between these genes.

3.2 Functional Analysis of TNBC-Related VIT Targets

To gain further insights into the functions of the 37 potential VIT target proteins, we performed GO enrichment and KEGG pathway analyses. The GO enrichment analysis identified a link between the proteins and important biological processes, such as transcription regulation, protein phosphorylation, neutrophil degranulation, peptidyl-threonine phosphorylation, and extracellular signal-regulated kinase 1 and 2 (ERK1 and ERK2) cascade regulation. In terms of cellular components, these proteins were found to be located in various areas, including the cytoplasm, cell surface, ficolin-1-rich granule lumen, nucleoplasm, and extracellular exosome. The proteins were primarily involved in functions such as transcription factor binding, protein serine/threonine kinase activity, Adenosine triphosphate (ATP) binding, protein kinase binding, and protein kinase activity, among others in the molecular function category (Fig. 1D).

The KEGG pathway analysis revealed that VIT in TNBC was associated with 67 signaling pathways ($p < 0.05$), with several of the top 20 pathways (Fig. 1E) found to be closely linked to tumor biology, including the HIF-1 signaling pathway, cell cycle regulation, autophagy, PD-L1 expression and the PD-1 checkpoint pathway in cancer, along with the thyroid hormone signaling pathway.

3.3 PPI Network Construction of TNBC-Related VIT Targets and Molecular Docking Validation

To illustrate the VIT hub targets and the effects on TNBC, we constructed a PPI network using the STRING database to obtain the potential protein interactions. As shown in Fig. 1F, *HIF-1A*, *CREEBP*, and *HSP90AA1* were selected as the VIT hub genes by analyzing the degrees between nodes.

To verify the reliability of the interaction between VIT and its potential hub genes, Libdock software was used to perform molecular docking. As depicted in Fig. 2A, we found that VIT forms hydrogen bonds with specific

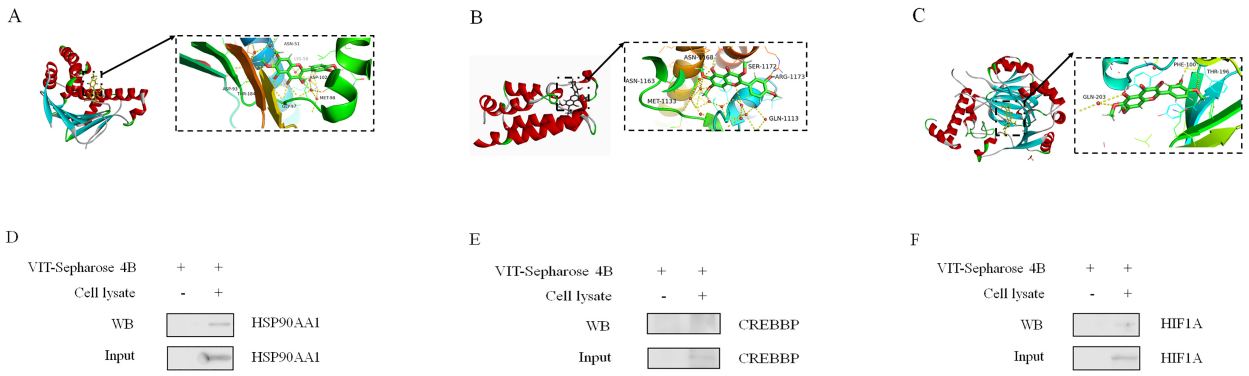

Fig. 2. Molecular docking validation and pull-down assay on potential VIT target genes in TNBC. (A) Intermolecular interactions by VIT with active site residues in HSP90AA1. (B) Intermolecular interactions by VIT with CREBBP active site residues. (C) Intermolecular interactions by VIT with HIF-1A active site residues. (D–F) The MDA-MB-231 cell lysates were incubated with Sepharose 4B-VIT beads and the pull-down proteins were analyzed by Western blot.

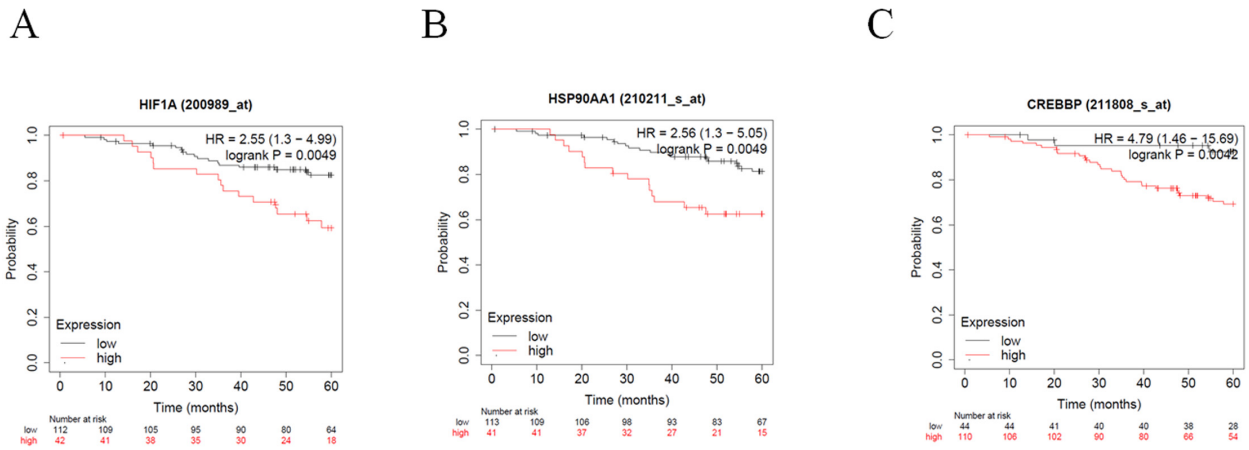

Fig. 3. The overall survival (OS) analysis of HSP90AA1, HIF-1A, and CREBBP by Kaplan–Meier. (A) The OS analysis for HIF-1A. (B) The OS analysis for HSP90AA1. (C) The OS analysis for CREBBP.

amino acid residues (ASN51, LYS58, ASP93, GLY97, and ASP102) in HSP90AA1, while also exhibiting attractive charge interactions with LYS58 in HSP90AA1. One carbon atom in VIT expressed the potential to form C–H bonds with the MET1133 amino acid residue in CREBBP (Fig. 2B). Analysis of the binding sites between VIT and HIF-1A demonstrated that VIT bound to the hydrophobic cavity of HIF-1A, with presented hydrogen bond featuring particularly prominently among the many interactions (PHE100, THR196, and GLN203) (Fig. 2C). Therefore, these results suggest that VIT might mainly act on HIF-1A, HSP90AA1, and CREEBP hub targets in treating against TNBC.

3.4 VIT Directly Binds with HIF-1A and HSP90AA1

To further identify the potential direct targets of VIT, Sepharose 4B–VIT beads were used in pull-down assays with MDA-MB-231 cell lysates. These results showed that VIT possessed a direct affinity to HSP90AA1 and HIF-1A but not with CREBBP (Fig. 2D–F).

3.5 Survival Analysis/Meta-Analysis of Potential VIT Hub Targets

To explore the clinical value of these three VIT hub target genes in TNBC, the Kaplan–Meier plotter online database was used to analyze disease-free survival. As shown in Fig. 3, the high expression of HSP90AA1, CREBBP, and HIF-1A was associated with poor overall survival (OS) for TNBC patients. These results found that the expression levels of HSP90AA1, CREBBP, and HIF-1A were significantly associated with the clinical prognosis of TNBC and may play key roles in the pathogenesis of TNBC.

3.6 VIT Inhibits Growth in TNBC Cell Lines MDA-MB-231 and HCC-1937

To evaluate the effect of VIT on cell proliferation, we performed a CCK8 assay using TNBC cell lines MDA-MB-231 and HCC-1937, which were treated with varying concentrations of VIT (ranging from 0 to 80 μM) for 24 h, 48 h, and 72 h. The results showed that the cell viabilities of

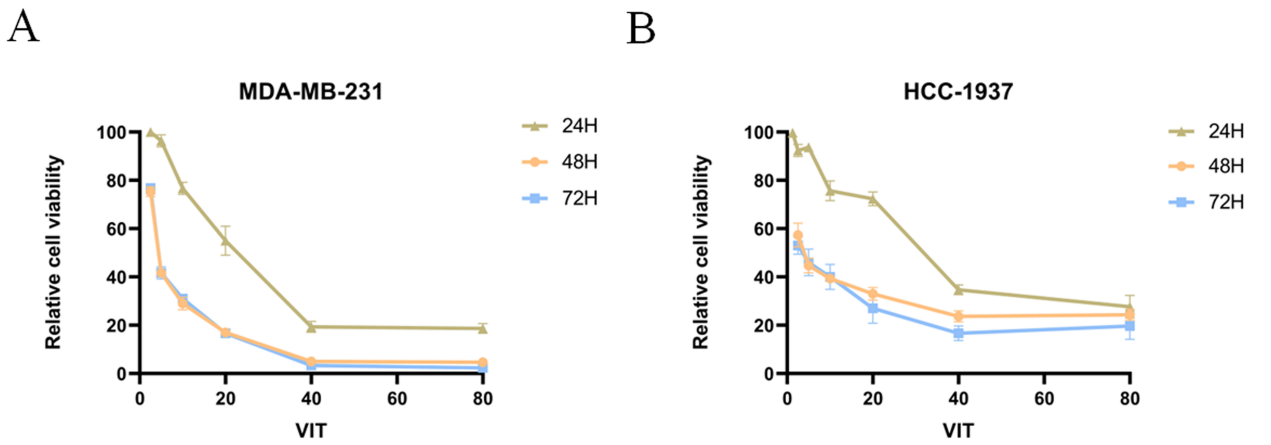

Fig. 4. Cell viability in MDA-MB-231 and HCC-1937 cells treated with VIT. (A) The effect of VIT on MDA-MB-231 cell growth. (B) The effect of VIT on HCC-1937 cell growth. The viability for each cell line was calculated using the Cell Counting Kit-8 (CCK-8) assay.

the MDA-MB-231 and HCC-1937 cell lines were decreased by VIT treatment in both a dose- and time-dependent manner (Fig. 4A,B, **Supplementary Fig. 1**). The IC_{50} values for VIT in the in MDA-MB-231 cells were determined at 24 h, 48 h, 72 h as 21.57 μM, 4.8 μM, and 4.8 μM, respectively. Whereas the respective values in the HCC-1937 cells were 31.60 μM, 3.86 μM, and 3.5 μM. Moreover, VIT presented with no cytotoxicity in normal HEK293T cells (**Supplementary Fig. 2**). Thus, these results indicate that VIT effectively inhibits the proliferation of TNBC cells in a concentration-dependent manner. In addition, the pharmacokinetic results found that many flavonoids reached maximum absorption at 24–36 h [10]. Therefore, we chose 1.25 μM, 5 μM, and 20 μM VIT concentrations to treat the MDA-MB-231 cells and concentrations of 3 μM, 10 μM, and 30 μM to treat the HCC-1937 cells, with a treatment period of 24 h chosen for both cell lines for future experiments.

3.7 VIT Induces Apoptosis and Promotes G2-Phase Cell Cycle Arrest in TNBC Cell Lines MDA-MB-231 and HCC-1937

The ability of VIT to induce apoptosis in MDA-MB-231 and HCC-1973 cells was detected by an Annexin V/ PI apoptosis assay using flow cytometry. In Fig. 5A–D, VIT efficiently induced apoptosis in both MDA-MB-231 and HCC-1937 cell lines in a dose-dependent manner. Apoptosis was observed in 20 μM (22.81%) VIT-treated MDA-MB-231 cells and in 30 μM (18.35%) VIT-treated HCC-1937 cells.

Then, we used PI staining to investigate whether VIT affects cell cycle progression. Fig. 5E,F demonstrate that the G2-phase distribution for MDA-MB-231 cells increased significantly as the VIT concentration increased and was accompanied by a decrease in the G1-phase distribution. This same situation was also reflected by HCC-1937 cells. In Fig. 5G,H, it can be seen that the G2-phase distribution for HCC-1937 cells also markedly increased, while the increase was more obvious in the initial low-concentration group. Moreover, the G2-phase distribution increased continuously as the VIT concentrations increased, while the G1-phase distribution significantly decreased. However, 30 μM of VIT simultaneously increased cell cycle arrest in the G2 phase and S phase. The results showed that VIT induced cell cycle arrest in the G2 phase in both the MDA-MB-231 and HCC-1937 cell lines.

3.8 VIT Downregulates the Expression of HSP90AA1, CREBBP, and HIF-1A in MDA-MB-231 and HCC-1937 Cells

Based on the results of the network pharmacology and molecular docking, we investigated whether VIT inhibited cell proliferation in TNBC through the hub genes; thus, we performed Western blotting to measure the expression of HSP90AA1, CREBBP, and HIF-1A in the MDA-MB-231 and HCC-1937 cell lines following incubation with VIT. As shown in Fig. 6, the protein levels of all three targets were significantly downregulated in the MDA-MB-231 and HCC-1937 cells after VIT treatment, in a concentration-dependent manner. These results illustrated that VIT inhibits the growth of TNCB cells by regulating its potential targets HSP90AA1, CREBBP, and HIF-1A.

4. Discussion

The conventional methods used to treat TNBC are surgery and chemotherapy, which can easily lead to poor clinical benefits owing to the development of drug resistance, recurrence, or metastasis [11]. Therefore, it is crucial to find a more effective treatment or drug candidate for TNBC. VIT, a natural flavonoid compound, was demonstrated to have a great effect on prostate carcinoma [12] and lung cancer [13]. The anti-tumor activity of VIT is attributed to its regulation of signaling pathways, such as Bcl-2, caspase, and HSP90, which promote apoptosis and

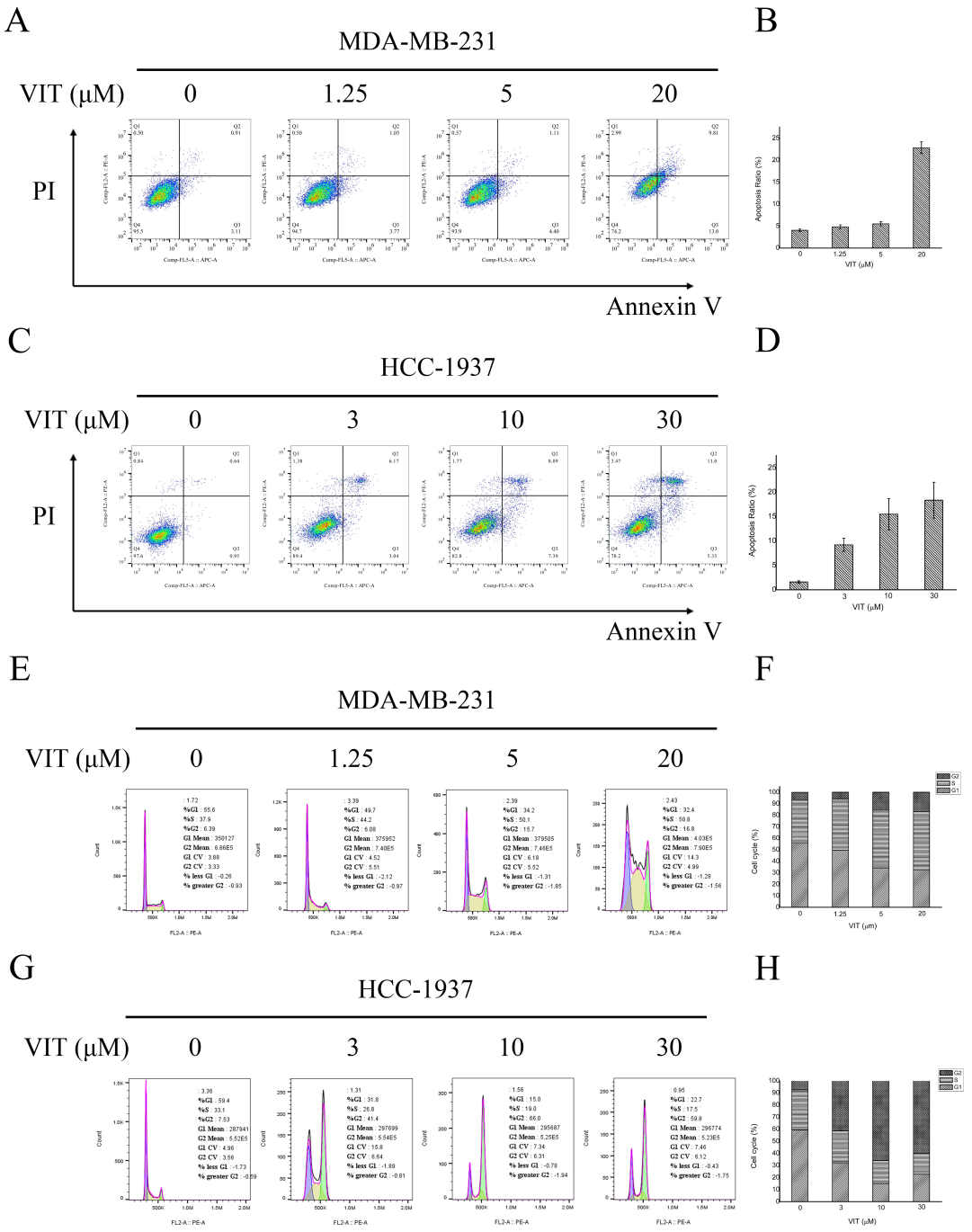

Fig. 5. Apoptosis and cell cycle analyses in MDA-MB-231 and HCC-1937 cells treated with VIT by flow cytometry. (A,B) The effect of VIT on apoptosis in MDA-MB-231 cells. (C,D) The effect of VIT on apoptosis in HCC-1937 cells. (E,F) The effect of VIT on cell cycle progression in MDA-MB-231 cells. (G,H) The effect of VIT on cell cycle progression in HCC-1937 cells.

induce the inhibition of proliferation and migration while promoting autophagy [14,15]. Moreover, the MEK/ERK, PI3K/AKT, and NF-κB pathways are blocked in response to the VIT treatment [16,17]. However, the specific mechanisms or potential targets of VIT in TNBC are yet to be studied deeply. In this study, we revealed the mechanisms of VIT for treating TNBC by integrating network pharmacology and *in vitro* experiments.

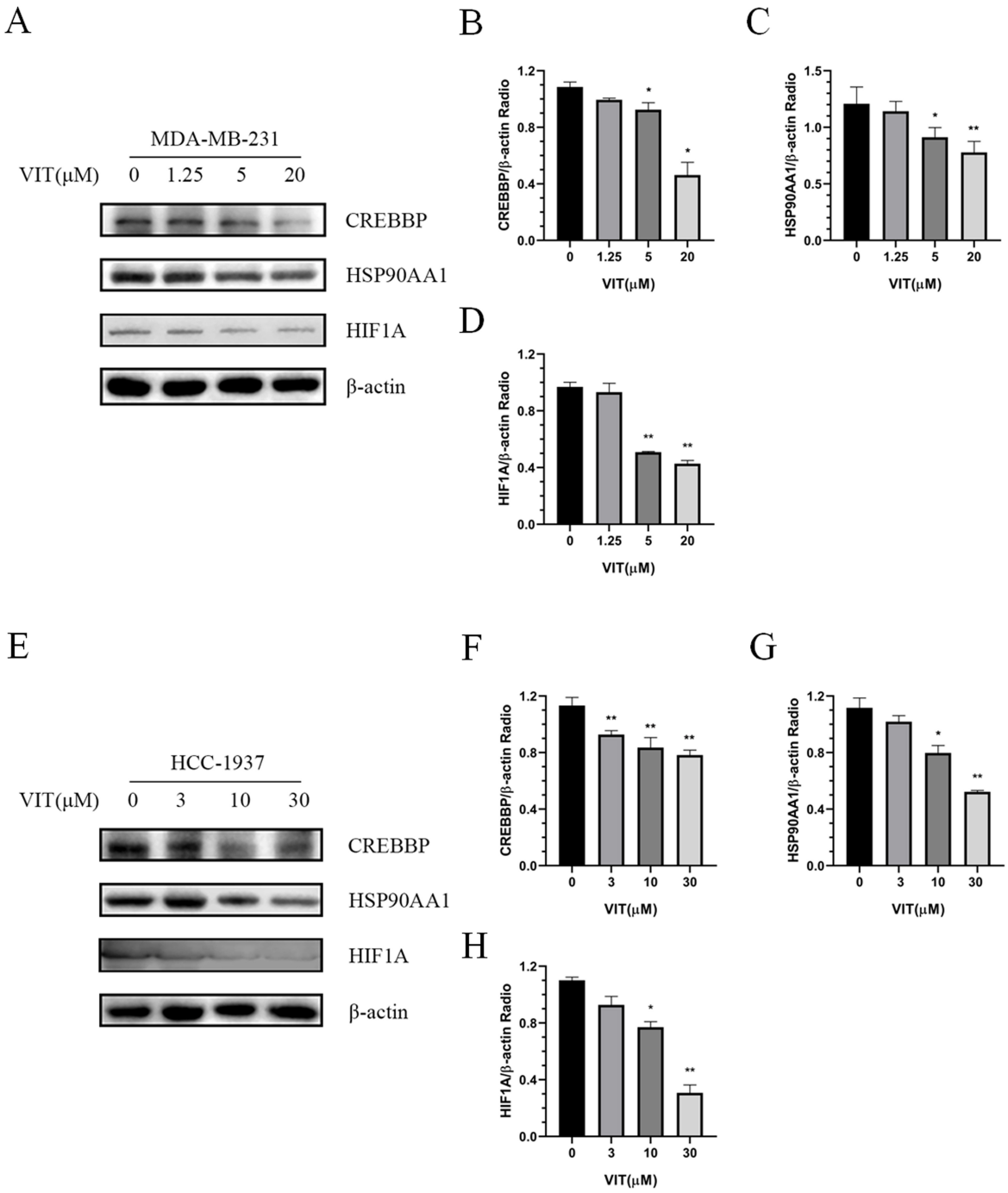

Fig. 6. Protein expression of CREBBP, HSP90AA1, and HIF-1A in VIT-treated cells. (A) MDA-MB-231 cells were treated with 1.25, 5, and 20 μM VIT for 24 hours to assess the expressions of CREBBP, HSP90AA1, and HIF-1A by Western blot analysis. (B–D) Relative expressions of CREBBP, HSP90AA1, and HIF-1A were analyzed by software Image J 1.54d (Wayne Rasband and contributors National Institutes of Health, USA). ** $p < 0.01$, * $p < 0.05$ *vs.* untreated group. (E) HCC-1937 cells were treated with 3, 10, and 30 μM VIT for 24 hours to assess the expressions of CREBBP, HSP90AA1, and HIF-1A by Western blot analysis. (F–H) Relative expressions of CREBBP, HSP90AA1, and HIF-1A were analyzed by Image J. ** $p < 0.01$, *$p < 0.05$ *vs.* untreated group.

In our study, 37 duplicated VIT and TNBC targets were found by network pharmacology analysis. Then, we used STRING to obtain the potential protein interactions and performed the biological functions of these targets using Cytoscape and the David database. The results indicated that these VIT targets are only involved in some pathways that are closely related to the development of TNBC, such as HIF-1, PD-1, and thyroid hormone pathways, and we predicted that HIF-1A, HSP90AA1, and CREBBP may target TNBC cells involved in the treatment of VIT.

Previous studies have found that HIF-1A, a key member of the HIF-1 family, is overexpressed in more than 80% of TNBC clinical cases and the HIF-1 pathway is hyperactivated in TNBC compared with other isotypes [18,19]. In our results, we showed that the expression of HIF-1A was associated with poorer overall survival in TNBC patients. Hence, HIF-1A has been considered a key biomarker for TNBC diagnosis and therapy. HIF-1A regulates multiple pathways and factors to modulate TNBC processes. Xu *et al*. [20] found that HIF-1A promotes TNBC tumorigenesis and procession by activating the WNT/β-catenin pathway. HIF-1A also controls the transcription of Bcl-2, Survivin, and X-linked inhibitor of apoptosis protein (XIAP) to influence the apoptosis of TNBC cells by initiating the cooperative binding of the C-TAD domain in HIF-1A and the co-activator CREBBP and p300. Past reports have revealed that CREBBP has critical roles in proliferation and cell cycle regulation [21–23]. Several reports have revealed that CREBBP is required for G1/S transition by regulating the E2F family in cancer cells [24,25]. CREBBP and its related paralog EP300 serve as transcriptional coactivators for the E2F transcription factor family, which play a central role in many genes that are required for G1/S transition to participate in the cancer phenotype [26,27]. Furthermore, CREBBP promotes H3K27 acetylation, resulting in the excessive repression of gene transcription and dysregulation [28,29]. The pull-down and Western blot (WB) results demonstrated that VIT binds directly to HIF-1A and decreases the expression of HIF-1A. However, there is no obvious interaction between VIT and CREBBP. These results demonstrate that VIT may be a potential inhibitor of HIF-1A, which can be used for TNBC treatment.

In response to tumor stimuli, the expression of HSP90AA1 is upregulated, and there is evidence linking HSP90AA1 to prognosis in colorectal cancer. Additionally, a notable association between HSP90AA1 and tumor stage has been observed in BRCA [30]. The Kaplan–Meier plotter results showed that the OS for TNBC with HSP90AA1 expression was low. These accumulating studies have indicated that HSP90AA1 has a pivotal effect in predicting TNBC development. From the previous experimental research, HSP90AA1 plays a key role in cell cycle regulation and DNA damage. Zhang *et al*. [31] explained that the lack of HSP90AA1 activity reduced cell displacement, which could be explained by the fact that cancer cells spend more time in the S/G2/M phases. Several studies have elucidated the relationship between HIF-1A and HSP90AA1: HIF-1A is regulated by HSP90 through RACK1 and interacts with Elongin C in a VHL-independent manner [32,33]. In this study, we demonstrated the direct binding between VIT and HSP90AA1 using pull-down assays, and we predicted the sites where VIT potentially binds to the active domain of HSP90AA1 by molecular docking. The effects are determined by Western blot, whereby VIT markedly reduces the expression of these targets.

In summary, we indicate that VIT reduces proliferation, induces apoptosis, and cell cycle arrest by targeting HSP90AA1 and HIF-1A, which leads to the inhibition of TNBC development and progression. These results suggest that VIT may be a potential therapeutic drug for treating TNBC.

5. Conclusions

VIT inhibited growth and induced apoptosis of TNBC cells by modulating HIF-1A, HSP90AA1, and CREBBP expression. Our findings suggest that VIT is a potential drug for TNBC therapy.

Availability of Data and Materials

The data that support the findings of this study are available from the corresponding author Dr. Weiqiang Guo, upon reasonable request.

Author Contributions

WG and YZ designed the research study and wrote the first manuscript. TW, YL, and DT performed *in vitro* experiments and data acquisition. MX and YG gave the Network pharmacology research. MS examined and explained the findings. Editorial revisions to the article were made with the participation of all writers. The final manuscript was reviewed and approved by all writers. All authors have participated sufficiently in the work to take public responsibility for appropriate portions of the content and agreed to be accountable for all aspects of the work in ensuring that questions related to its accuracy or integrity.

Ethics Approval and Consent to Participate

Not applicable.

Acknowledgment

Not applicable.

Funding

The present study was supported by the National Science Foundation of China (81502958), Minsheng Science and Technology Project of Suzhou (SS202086, SKJY2021032), and the Technology innovation team of Synthesis and research of Small Molecule targeted Anticancer drugs (SZWZYTD202204).

Conflict of Interest

The authors declare no conflicts of interest.

Supplementary Material

Supplementary material associated with this article can be found, in the online version, at https://doi.org/10.31083/j.fbl2812341.

References

[1] Siegel RL, Miller KD, Fuchs HE, Jemal A. Cancer Statistics, 2021. CA: A Cancer Journal for Clinicians. 2021; 71: 7–33.

[2] Yin L, Duan JJ, Bian XW, Yu SC. Triple-negative breast cancer molecular subtyping and treatment progress. Breast Cancer Research: BCR. 2020; 22: 61.

[3] Singh DD, Yadav DK. TNBC: Potential Targeting of Multiple Receptors for a Therapeutic Breakthrough, Nanomedicine, and Immunotherapy. Biomedicines. 2021; 9: 876.

[4] Bianchini G, Balko JM, Mayer IA, Sanders ME, Gianni L. Triple-negative breast cancer: challenges and opportunities of a heterogeneous disease. Nature Reviews. Clinical Oncology. 2016; 13: 674–690.

[5] Ganesan K, Xu B. Molecular targets of vitexin and isovitexin in cancer therapy: a critical review. Annals of the New York Academy of Sciences. 2017; 1401: 102–113.

[6] He M, Min JW, Kong WL, He XH, Li JX, Peng BW. A review on the pharmacological effects of vitexin and isovitexin. Fitoterapia. 2016; 115: 74–85.

[7] Zhang G, Li D, Chen H, Zhang J, Jin X. Vitexin induces G2/M phase arrest and apoptosis via Akt/mTOR signaling pathway in human glioblastoma cells. Molecular Medicine Reports. 2018; 17: 4599–4604.

[8] Zhang R, Zhu X, Bai H, Ning K. Network Pharmacology Databases for Traditional Chinese Medicine: Review and Assessment. Frontiers in Pharmacology. 2019; 10: 123.

[9] Lánczky A, Győrffy B. Web-Based Survival Analysis Tool Tailored for Medical Research (KMplot): Development and Implementation. Journal of Medical Internet Research. 2021; 23: e27633.

[10] Ross JA, Kasum CM. Dietary flavonoids: bioavailability, metabolic effects, and safety. Annual Review of Nutrition. 2002; 22: 19–34.

[11] Nedeljković M, Damjanović A. Mechanisms of Chemotherapy Resistance in Triple-Negative Breast Cancer-How We Can Rise to the Challenge. Cells. 2019; 8: 957.

[12] Song L, Chen X, Mi L, Liu C, Zhu S, Yang T, *et al*. Icariin-induced inhibition of SIRT6/NF-κB triggers redox mediated apoptosis and enhances anti-tumor immunity in triple-negative breast cancer. Cancer Science. 2020; 111: 4242–4256.

[13] Katz H, Alsharedi M. Immunotherapy in triple-negative breast cancer. Medical Oncology (Northwood, London, England). 2017; 35: 13.

[14] Meng FM, Yang JB, Yang CH, Jiang Y, Zhou YF, Yu B, *et al*. Vitexicarpin induces apoptosis in human prostate carcinoma PC-3 cells through G2/M phase arrest. Asian Pacific Journal of Cancer Prevention: APJCP. 2012; 13: 6369–6374.

[15] Gong Q, Cao X, Cao J, Yang X, Zeng W. Casticin suppresses the carcinogenesis of small cell lung cancer H446 cells through activation of AMPK/FoxO3a signaling. Oncology Reports. 2018; 40: 1401–1410.

[16] Vo GV, Nguyen THT, Nguyen TP, Do THT, Tran NMA, Nguyen HT, *et al*. *In silico* and *in vitro* studies on the anti-cancer activity of artemetin, vitexicarpin and penduletin compounds from *Vitex negundo*. Saudi Pharmaceutical Journal: SPJ: the Official Publication of the Saudi Pharmaceutical Society. 2022; 30: 1301–1314.

[17] Lee CY, Chien YS, Chiu TH, Huang WW, Lu CC, Chiang JH, *et al*. Apoptosis triggered by vitexin in U937 human leukemia cells via a mitochondrial signaling pathway. Oncology Reports. 2012; 28: 1883–1888.

[18] Zheng XX, Zhang RS, Zhou YJ, Wang JG. Role of ERK/FoxO3a signal axis in inhibitory effect of vitexin 1 (VB-1) in HepG2 cell proliferation. Zhongguo Zhong Yao Za Zhi. 2014; 39: 1276–1279.

[19] Surh Y. Cancer chemoprevention with dietary phytochemicals. Nature Reviews Cancer. 2003; 3: 768–780.

[20] Xu R. P4HA1 is a new regulator of the HIF-1 pathway in breast cancer. Cell Stress. 2019; 3: 27–28.

[21] Liu Q, Guan C, Liu C, Li H, Wu J, Sun C. Targeting hypoxia-inducible factor-1alpha: A new strategy for triple-negative breast cancer therapy. Biomedicine & Pharmacotherapy. 2022; 156: 113861.

[22] Liu X, Xie P, Hao N, Zhang M, Liu Y, Liu P, *et al*. HIF-1-regulated expression of calreticulin promotes breast tumorigenesis and progression through Wnt/β-catenin pathway activation. Proceedings of the National Academy of Sciences of the United States of America. 2021; 118: e2109144118.

[23] Goodman RH, Smolik S. CBP/p300 in cell growth, transformation, and development. Genes & Development. 2000; 14: 1553–1577.

[24] Ait-Si-Ali S, Polesskaya A, Filleur S, Ferreira R, Duquet A, Robin P, *et al*. CBP/p300 histone acetyl-transferase activity is important for the G1/S transition. Oncogene. 2000; 19: 2430–2437.

[25] Trouche D, Kouzarides T. E2F1 and E1A(12S) have a homologous activation domain regulated by RB and CBP. Proceedings of the National Academy of Sciences of the United States of America. 1996; 93: 1439–1442.

[26] Wang H, Larris B, Peiris TH, Zhang L, Le Lay J, Gao Y, *et al*. C/EBPbeta activates E2F-regulated genes *in vivo* via recruitment of the coactivator CREB-binding protein/P300. The Journal of Biological Chemistry. 2007; 282: 24679–24688.

[27] Zhang J, Vlasevska S, Wells VA, Nataraj S, Holmes AB, Duval R, *et al*. The CREBBP Acetyltransferase Is a Haploinsufficient Tumor Suppressor in B-cell Lymphoma. Cancer Discovery. 2017; 7: 322–337.

[28] Wei W, Song Z, Chiba M, Wu W, Jeong S, Zhang JP, *et al*. Analysis and therapeutic targeting of the EP300 and CREBBP acetyltransferases in anaplastic large cell lymphoma and Hodgkin lymphoma. Leukemia. 2023; 37: 396–407.

[29] Jiang M, Yan Y, Yang K, Liu Z, Qi J, Zhou H, *et al*. Small molecule nAS-E targeting cAMP response element binding protein (CREB) and CREB-binding protein interaction inhibits breast cancer bone metastasis. Journal of Cellular and Molecular Medicine. 2019; 23: 1224–1234.

[30] Liu H, Zhang Z, Huang Y, Wei W, Ning S, Li J, *et al*. Plasma HSP90AA1 Predicts the Risk of Breast Cancer Onset and Distant Metastasis. Frontiers in Cell and Developmental Biology. 2021; 9: 639596.

[31] Zhang T, Zhu X, Wu H, Jiang K, Zhao G, Shaukat A, *et al*. Targeting the ROS/PI3K/AKT/HIF-1α/HK2 axis of breast cancer cells: Combined administration of Polydatin and 2-Deoxy-d-glucose. Journal of Cellular and Molecular Medicine. 2019; 23: 3711–3723.

[32] Neckers L, Ivy SP. Heat shock protein 90. Current Opinion in Oncology. 2003; 15: 419–424.

[33] de Heer EC, Jalving M, Harris AL. HIFs, angiogenesis, and metabolism: elusive enemies in breast cancer. The Journal of Clinical Investigation. 2020; 130: 5074–5087.